This author accepted manuscript is deposited under a Creative Commons Attribution Non-commercial 4.0 International (CC BY-NC) licence. This means that anyone may distribute, adapt, and build upon the work for non-commercial purposes, subject to full attribution. If you wish to use this manuscript for commercial purposes, please visit Marketplace.

Postprint of: Kostro G., Michna M., Kutt F. and Ryndzionek R., Improved methods for stator end winding leakage inductance calculation, COMPEL - The international journal for computation and mathematics in electrical and electronic engineering, Vol. 42 No. 4 (2023), pp. 972-980. DOI: 10.1108/COMPEL-09-2022-0330

# Improved Methods for Stator End Winding Leakage Inductance Calculation

Kostro Grzegorz, Michna Michał, Kutt Filip, Ryndzionek Roland

Gdańsk University of Technology, Faculty of Electrical and Control Engineering 11/12 Gabriela Narutowicza Street, Gdansk, Poland, e-mail: grzegorz.kostro@pg.edu.pl

Abstract - This paper proposes improved methods for calculating the value of the stator end winding leakage inductance of an induction machine. The forms were based on the stored magnetic energy, calculated by 3-D finite element analysis. In these methods, the rotor has been considered in the simulated machine's model. The analysis results show that the stator end winding leakage inductance value is a significant part of the value of the total leakage inductance. Therefore, considering end winding leakage inductance in a dynamic induction machine model improves the model accuracy.

**Purpose** - Calculating the stator end-winding leakage inductance, taking into account the rotor, is difficult due to the irregular shape of the end-winding. The end-winding leakage may distribute at the end of the active part and the fringing flux of the air gap. The fringing flux belongs to the main flux but goes into the end-winding region. Then, not all the magnetic flux occurring in the end region is the end-winding leakage flux. Therefore, it is essential to find a method to accurately separate the leakage from the total flux, taking into account the rotor.

**Design/methodology/approach** - In this paper, two methods based on energy calculation are presented. Both methods require the assumption that the machine is symmetrical. The first method depends on the total leakage inductance and the machine's active region length. The second method is based on the energy stored in the end region of the machine. In this case, removing the energy produced by the fringing flux of the air gap is necessary. The model should have a volume-closing fringing flux to remove the part of energy belonging to the end of the air gap.

**Findings** - The method presented in the paper does not require rotor removal. The values of the end-winding leakage inductance computed based on the proposed method were compared with values computed using the method with the removed rotor. The computations show that the proposed method is closest to the results from the method presented in the literature. Results obtained in the first method present that rotor influence on the value of end-winding leakage inductance exists. The model of the stator end-winding described in the paper is general. Therefore the proposed methods are suitable for calculating the end-winding leakage inductance of other electric machines.

**Originality/value** - The method presented in the paper considers the rotor in end-winding leakage inductance calculation. It is not necessary to remove the rotor as in the similar method presented in the literature. The authors elaborated a parametric model with a volume-closing fringing flux to remove the part of energy belonging to the end of the air gap. The authors also elaborated their 3D model of the machine Winding for calculations in Opera 3D.

Keywords: leakage field, finite element method, electrical machines.

**Article Type**: Research paper

#### I. INTRODUCTION

The magnetic flux produced by the currents flowing through the windings of the electric machine can be divided into two components. The first magnetic flux component produced by the currents flowing through the end-windings is usually termed end-winding leakage flux. The main flux is the second component produced by the currents flowing through conductors placed in the machine's active part. Although the end-winding leakage flux is small in comparison with the main flux, it may cause some harmful phenomena, such as magnetic forces on the end-winding (Kim et al., 2005), (Fang et al., 2013), (Lin and Arkkio, 2008), (Stancheva and Iatcheva, 2009), and the eddy currents in the conductive parts on the end region (Yao et al., 2006), (Lin at al., 2010) and in the

core end (Yamazaki at al., 2008). Besides, the accurately determined value of the leakage inductance is essential when calculating the induction motor's starting torque and current.

The geometry of the end part is more complex than the geometry of the active part. In the active part, the magnetic flux density vector may be represented by a 2-D vector rotated in the plane of magnetic core laminations (Guo et al., 2008). However, the magnetic flux density distribution in the machine's end part is always 3-D, and thus the analysis of this part is more complex and time-consuming.

## II. SURVEY OF RELATED WORKS

Mainly there are two approaches to calculating the value of end-winding leakage inductance. One approach is based on the magnetic energy stored in the end region (Brahimi et al., 1992), (Arshad et al., 2005), (De Weerdt et al., 1997), (De Weerdt and Belmans, 1995), and the other is based on the flux leakage linking with the end-winding (Lin and Arkkio, 2009), (Meessen et al., 2008), (Hsieh at al., 2007). Numerical methods, such as the finite element method (FEM), and two analytical methods, e.g., equivalent magnetic circuits (Meessen et al., 2008) and Neumann integral (Ban et al., 2003), (Freese, 2010), (Freese and Kulig, 2012), (Schramm and Gerling, 2005), have been used to calculate the above quantities.

An analytical calculation presented by (Hsieh et al., 2007) is based on solving the flux linkage. The geometry of the end-winding was modeled as a semicircle, the method gave the rough value of the end-winding inductance, but it was fast. Another analytical approach (Ban et al., 2003), (Freese, 2010), (Freese and Kulig, 2012), using the method of images,

took into account the influence of the iron core. The end-winding was modeled by 3-D diamond Winding to solve the problem.

In (De Weerdt et al., 1997) and (Weerdt and Belmans, 1995), the end-winding inductance was calculated using 2-D and 3-D models. The 2-D model calculated the end ring inductance under different boundary conditions. The leakage inductance calculations with different degrees of coupling between the rotor and stator were based on the energy calculated utilizing the 3D model.

The 3D finite element analysis (FEA) gives accurate results. However, it is very time-consuming and requires many computation steps. The analyzed model has to be reduced to make it less time-consuming. It is necessary to assume that the machine is axis-symmetric. In addition, a quasi-3-D FEA requires the assumption that the field variables are sinusoidally distributed along the circumferential direction.

This paper proposes improved methods for calculating the stator end-winding leakage inductance.

#### III. RESEARCH METHODS

Due to the irregular shape of the end-winding, the stator end-winding leakage inductance must consider that the rotor is rugged. The end-winding leakage may distribute at the end of the active part and the fringing flux of the air gap. The fringing flux belongs to the main flux but goes into the end-winding region. Then, not all the magnetic flux occurring in the end region is the end-winding leakage flux. Therefore, it is essential to find a method to separate the leakage from the total flux accurately.

In this paper, two methods based on energy calculation are presented. Both methods require the assumption that the machine is symmetrical.

The first method, which will be called method A is based on the dependence between the total inductance and the length of the machine's active region, and it can be written as follows:

$$L_{tot} = L_{active} + L_{send}$$
 (1)

 $L_{active}$  is proportional to the axial length of the active motor part  $(l_{Fe})$ , and  $L_{\sigma end}$  remains constant and is independent of  $l_{Fe}$ .

The total inductance is calculated for a few lengths of the active region. The total inductance is divided into two parts using extrapolation of the total inductance value into the iron length equal to zero. The method is similar to the method presented in the literature (Lin and Arkkio, 2009). The currents applying to the model produce fluxes in opposite directions in neighboring winding; the energy stored in the volume of the model is proportional to the total inductance. Then, the inductance can be calculated from the formula:

$$L_{tot} = \frac{4 \cdot E_{tot}}{2 \cdot I_{pli}^2} \tag{2}$$

Where:  $L_{tot}$  total inductance,  $E_{tot}$  energy stored in the volume of the model,  $I_{ph}$  current applied through the

windings.

The second method will be called method B based on the energy stored in the end region of the machine. In this case, removing the energy produced by the fringing flux of the air gap is necessary. The model should have a volume-closing fringing flux to remove the part of energy belonging to the end of the air gap. The authors assumed that the volume has a ring shape. The dimensions of the ring can be obtained from the formulas:

$$D_{in} = D_r - h_r. (3)$$

$$D_{out} = D_s + h_s. (4)$$

$$h = (D_s - D_r) \cdot k_c. \tag{5}$$

Where:  $D_{in}$  inner diameter of the ring,  $D_r$  diameter of the rotor,  $h_r$  height of rotor slot opening,  $D_{out}$  outer diameter of the ring,  $D_s$  stator inner diameter,  $h_s$  height of stator slot opening, h height of the ring,  $k_c$  Carter coefficient. The dimensions of the ring were determined on the base of magnetic flux density analysis in the volume where the fringing flux is present. The view of the motor model with the ring mentioned above is shown in Fig. 1.

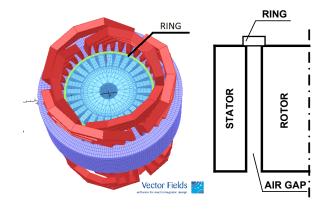


Fig.1. View of the 3D motor model with ring used in method B and sketch of its cross-section

In method B the value of end winding leakage inductance is calculated from formula:

$$L_{gend} = \frac{4 \cdot E_{EndReg}}{3 \cdot I_{ph}^2}$$
(6)

Where:  $L_{\sigma end}$  is end-winding leakage inductance,  $E_{EndReg}$  energy stored in the volume of the end region,  $I_{ph}$  current applied through the windings.

Method B is less time-consuming than method A because the value of end-winding inductance is calculated directly from energy. Method B does not require additional calculations or mathematical operations like method A. Both presented methods can be used to improve the accuracy of a dynamic model of an induction machine.

Energy calculation for both methods was made using VECTOR FIELDS software called OPERA 3D. It required 3D windings and magnetic core models.



## III. FINITE ELEMENT MODEL OF THE MOTOR

Using the coil models from the standard library of OPERA to build the stator winding with a significant filling factor can cause dimensional conflicts in the end-winding part (coils in the end-winding part overlap each other). Therefore such models lead to changes in the flux density distribution in the end-winding region. The consequence of this is erroneous in specifying the value of end-winding inductance. Therefore, it is necessary to develop models of coils that allow the construction of a winding without dimensional conflicts.

It should be noted that constructing coil models of any shape is possible in Opera 3D. For this purpose, the standard conductors from OPERA's library (bricks described by 8 and 20 node elements) can be used. The computer program was developed to automate building the AC machine's stator windings, using the 8-node elements to construct stator winding. The geometric model of the considered coil is defined by two basic objects (Fig. 2): a longitudinal coil axis and a set of cross-sections corresponding to the number of points defining a longitudinal axis of the coil.

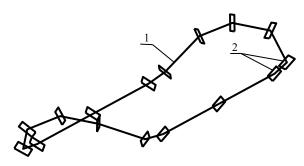


Fig. 2. Model 3D of a stator winding coil of an electric machine:  $1-\log$  longitudinal coil axis, 2- set of transverse coil cross-section

Fig. 3 shows an example of a complete stator winding model built using the developed program.

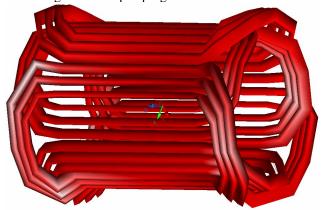


Fig. 3. Model 3D of single layer stator winding of an electric machine with concentrically wound coils

It should be noted that the construction of the model coil using the library 8-node elements requires the assumption of appropriate current density in the individual segments of the

coil. The total current of the modeled coil in 3D Opera is a product of the assumed value of the current density and the area of the bottom base of the 8-node element (rectangle defined as the first). The direction of current flow determines the vector acting at the bottom base's geometric center and directed to the upper base of the 8-node element.

The current density has the same value in each segment of the coil will cause the values of total currents in each of these elements to be different since the total current for the elements having the same cross-sectional area and the same density may take different values depending on the value of the bottom base area. It results in errors in flux density distribution calculation.

The OPERA 3D has two modules for constructing a geometric model of the analyzed object: the modeler module and the Pre-Processor module. Due to the greater possibility of changing the mesh density in the analyzed object, the authors have used the Pre-Processor module. However, it should be noted that the construction of a discrete model of the motor using this module is very time-consuming and requires much work. In order to shorten the construction time of a discrete model of the machine, the authors developed a unique computer program. This program can build a model based on basic geometric dimensions (slot dimensions, stator outer diameter, the inner diameter of the stator, rotor diameter, the length of the active part, etc.) and the number of slots. A discrete model of the 3D motor used to calculate its windings inductance is shown in Fig. 4.

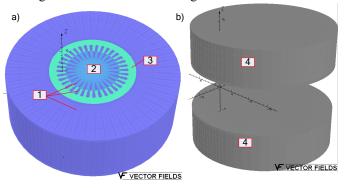


Fig. 4. Geometrical model of the considered motor made utilizing OPERA Pre-Processor: a) 3D model of the machine active part, air (1), rotor (2), stator (3), b) model of the end-winding background, air (4)

## IV. STATOR END-WINDING LEAKAGE INDUCTANCE

The value of the end-leakage inductance was calculated for a 2.2 kW squirrel cage asynchronous motor. The main specification of the simulated machine is listed in Table I.

Calculations were carried out using the TOSCA module. In the calculations was assumed constant permeability of magnetic circuit of the motor ( $\mu_r$ =500) and the currents value were as follows: the current in the first phase was equal to  $I_{ph}$ , and in the other two phases was equal to -0.5 $I_{ph}$ .

The total energy calculated using method A for different lengths of active machine parts is listed in Table II.



TABLE I
MAIN SPECIFICATION OF SIMULATED MACHINE

Name	Value
Rated power (kW)	2.2
Rated frequency (Hz)	50
Total length of stator iron core (mm)	100
Outer diameter of stator iron core (mm)	97
Inner diameter of stator iron core (mm)	47
Thickness of air gap (mm)	0.15
Number of pole pairs	2
Number of stator slots	36
Number of rotor slots	28
Number of parallel branches	1
Number of turns in series in a stator coil	39
Coil span of a stator coil (stator slot pitches	7, 9, 11

The total energy calculated using method A for different lengths of active machine parts is listed in Table II.

TABLE II
THE ENERGY OF SIMILATED MACHINE - METHOD A

THE ENERGY OF SIMULATED MACHINE – METHOD A	
Active part length (mm)	Stored Energy (J) <sup>a</sup>
100	0.37693
90	0.33961
80	0.30229
70	0.26497
60	0.22765

The dependence of the total inductance on its active part length is shown in Fig.5.

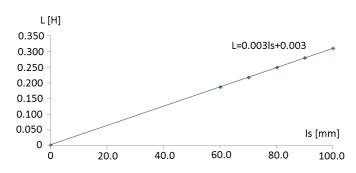


Fig. 5. The dependence of the total inductance from its active part length  $l_s$ 

The value of the end-winding leakage inductance was calculated using the least mean square method on the base of energy values presented in Table II. Method A gives the value of the end-winding leakage inductance equal to 3.06mH.

The energy value stored in the simulated model's end region calculated using method B for  $I_{Fe}$  equal to 100mm is 4.32mJ, and the corresponding end-winding leakage inductance calculated using equation (2) is 3.5mH. To verify the values of end-winding inductance calculated by methods A and B author compared these values with the inductance value calculated based on the method with the removed rotor (Arshad et al., 2005), (De Weerdt et al., 1997), (De Weerdt and Belmans, 1995). The end-winding leakage inductance value for the model with a removed rotor equals 3.6 mH.

Method A requires significant accuracy in Energy calculation due to the big difference between energy stored in the active part and the end-winding part of the machine.

## V. CONCLUSIONS

This paper proposes improved methods for calculating a rotating electric motor's end-winding leakage inductance. The stator end-winding leakage inductance of the 2.2-kW induction motor was computed based on the proposed methods. The method presented in the paper does not require rotor removal. The values of the end-winding leakage inductance computed based on the proposed method were compared with values computed using the method with the removed rotor. The computations show that method B is closest to the results from the method presented in the literature.

The difference between end-winding leakage inductance calculated using methods A and B is less than 20%.

Results obtained in method A show that rotor influence on the value of end-winding leakage inductance exists. The difference between end-winding leakage inductance calculated using method A and the method that requires rotor removal is 17%.

The model of the stator end-winding described in the paper is general. Therefore the proposed methods are suitable for calculating the end-winding leakage inductance of other radial flux electric machines.

## REFERENCES

Arshad W. M., Lendenmann H., Liu Y., Lamell J.-O., and Persson H. (2005), "Finding end winding inductances of MVA machines," in Industry Applications Conference, 2005. Fourtieth IAS Annual Meeting. Conference Record of the 2005, vol. 4, pp. 2309–2314.

Ban D., Zarko D., and Mandic I. (2003), "Turbogenerator end winding leakage inductance calculation using a 3-D analytical approach based on the solution of Neumann integrals," in Electric Machines and Drives Conference, 2003. IEMDC'03. IEEE International, 2003, vol. 3, pp. 1576–1582 vol.3.

Brahimi A., Foggia A., and Meunier G. (1992), "End Winding Reactance Computation Results Using a 3D Finite Element Program," in Digest of the Fifth Biennial IEEE Conference on Electromagnetic Field Computation, pp. TP23–TP23.

De Weerdt R. and Belmans R. (1995), "Squirrel cage induction motor end effects using 2D and 3D finite elements," in Electrical Machines and Drives, 1995. Seventh International Conference on (Conf. Publ. No. 412), pp. 62–66. De Weerdt R., Tuinman E., Hameyer K., and Belmans R. (1997), "Finite element analysis of steady state behavior of squirrel cage induction motors compared with measurements," IEEE Trans. Magn., vol. 33, no. 2, pp. 2093–2096.

Fang Y., Lv Q., Cheng X., and Bao X. (2013), "Analysis of stress distribution on end winding of large water filling submersible motor during steady-state operation," in 2013 5th International Conference on Power Electronics Systems and Applications (PESA), pp. 1–6.

Freese M. (2010), "Analytic Calculation of Turbo Generator End Winding Inductances using Neumann's Formula", *International Symposium on Power Electronics, Electrical Drives, Automation and Motion (SPEEDAM)*, Italy 2010, pp. 1597 – 1602.

Freese M., Kulig S. (2012), "Influence of constructional turbo-generator end region design on end winding inductances", Archives of Electrical Engineering vol. 61(2), 2012, pp. 199-210.

Guo Y., Zhu J. G., Zhong J., Lu H., and Jin J. X. (2008), "Measurement and Modeling of Rotational Core Losses of Soft Magnetic Materials Used in Electrical Machines: A Review," IEEE Trans. Magn., vol. 44, no. 2, pp. 279–291.



Hsieh M.-F., Hsu Y.-C., Dorrell D. G., and Hu K.-H. (2007), "Investigation on End Winding Inductance in Motor Stator Windings," IEEE Trans. Magn., vol. 43, no. 6, pp. 2513–2515.

Kim K.-C., Lee H.-W., Chun Y.-D., and Lee J. (2005), "Analysis of electromagnetic force distribution on end winding for motor reliance," IEEE Trans. Magn., vol. 41, no. 10, pp. 4072–4074.
Lin R. and Arkkio A. (2008), "3-D Finite Element Analysis of Magnetic

Forces on Stator End-Windings of an Induction Machine," IEEE Trans. Magn., vol. 44, no. 11, pp. 4045-4048.

Lin R. and Arkkio A. (2009), "Calculation and Analysis of Stator End-Winding Leakage Inductance of an Induction Machine," IEEE Trans. Magn., vol. 45, no. 4, pp. 2009-2014.

Lin R., Haavisto A., and Arkkio A. (2010), "Analysis of Eddy-Current Loss in End Shield and Frame of a Large Induction Machine," IEEE Trans. Magn., vol. 46, no. 3, pp. 942–948.

Meessen K. J., Thelin P., Soulard J., and Lomonova E. (2008), "Inductance Calculations of Permanent-Magnet Synchronous Machines Including Flux Change and Self- and Cross-Saturations," IEEE Trans. Magn., vol. 44, no. 10, pp. 2324-2331.

Schramm A. and Gerling D. (2005), "Analytical calculation of the end winding leakage inductance based on the solution of Neumann integrals," in Proceedings of the IEEE International Symposium on Industrial Electronics, 2005. ISIE 2005, vol. 2, pp. 851-855 vol. 2.

Stancheva R. D. and Iatcheva I. (2009), "3-D Electromagnetic Force Distribution in the End Region of Turbogenerator," IEEE Trans. Magn., vol. 45, no. 3, pp. 1000-1003.

Yamazaki K., Tada S., Mogi H., Mishima Y., Kaido C., Kanao S., Takahashi K., K. Ide, Hattori K., and Nakahara A. (2008), "Eddy Current Analysis Considering Lamination for Stator Core Ends of Turbine Generators," IEEE Trans. Magn., vol. 44, no. 6, pp. 1502–1505.

Yao Y., Xia H., Ni G., Liang X., Yang S., and Ni P. (2006), "3-D eddy current analysis in the end region of a turbogenerator by using reduced magnetic vector potential," IEEE Trans. Magn., vol. 42, no. 4, pp. 1323-1326.

